Expanding A Semiclassical Approach to the Non-Interacting Atom

Jeremy Ovadia

May 29, 2009

Contents

Abstract

A thorough understanding of the scaling, energy, and density of the an atom with non-interacting electrons is revealed. By further expanding Englert's rate in which the electrons fill the shells, $y(N)$, sharp bounds for the energy and an exact energy density are developed and the chemical potential and ionization energy are studied. The scaled quantum corrections of this electronic system are explored and modeled as a sequence of functions uniformly converging to the difference between Heilmann and Lieb's hydrogenic density, $\rho^H(r)$, and an infinite Thomas-Fermi density. Also, implications of what may be carried over to the real atom are discussed.

Supervised by: Kieron Burke, Department of Chemistry & Physics

Chapter 1

Introduction

1.1   Background

Originating in the 1920s, the Thomas-Fermi theory gave birth to DFT and was used as an initial approximation for functionals [1]. By examining an electronic system as a slowly varying homogeneous gas, the Thomas-Fermi approximation treats an electronic system without the quantum effect of shell structure and becomes relatively exact as the system becomes large [2]. The Thomas-Fermi theory provides computationally cheap approximations due to its relatively simple structure. However through the improvement upon the accuracy of Kohn-Sham self-consistent field theory (SCF), it is often only used in particular cases with larger number of particles for which general gradient approximations, Monte Carlo and Hartree-Fock methods are too costly [3].

Modern DFT instead has primarily expanded upon the Kohn-Sham SCF theory where the Kohn-Sham equations map an interacting electronic system with some external potential exactly to a new non-interacting electronic system with an effective potential defined to reproduce the exact density accompanied by exchange and correlation energies [4]. Exact functionals for the exchange and correlation energies are still unknown and can only be approximated as of now. It follows that DFT has become an approach in electronic structure theory where better approximations are continuously sought.

Although Kohn-Sham SCF theory has become widespread in DFT, Kohn and Sham developed Kohn-Sham Green's Function (GF) theory that does not use the Kohn-Sham equations but instead improves approximations made by Thomas-Fermi theory. Using semiclassical methods, such as the Wentzel-Kramers-Brillouin (WKB) approximation for wavefunctions, to improve upon gradient expansion theory and complicated Green's Functions, Kohn-Sham GF theory provides highly accurate quantum corrections to Thomas-Fermi approximations and a fundamentally different approach to traditional views of Kohn-Sham SCF theory [5].

Kohn-Sham GF theory has lacked popularity in the development of DFT due to successes of generalized gradient approximations [6], however recent improvements within it have been constructed and quantum corrections have been further understood such that closed forms for some non-interacting systems can be achieved [7]. Due to this promise within these Kohn-Sham GF theory improvements, we study a simple electronic system and develop a model for its density: the non-interacting atom.

The non-interacting atom as an electronic system stands very different from the real atom, but some material we can obtain from the non-interacting atom should be able to

provide us information for the real atom. First, the non-interacting atom has a $-Z/r$ potential just like the real atom and not the effective potential of the real atom, so the Kohn-Sham equations cannot be simply applied to map information on the non-interacting atom to the real atom. The orbitals of each of these atoms also fill in different fashions which stands evident in the manner in which the real atom fills its $3p$ and its $4s$ orbitals in succession while the non-interacting atom fills its $3d$ orbital after its $3p$ orbital.

Even so, some material from the non-interacting atom could help understand how to approach the real atom, methodology of the real atom, or some results may be applicable for both real and non-interacting atoms. The Thomas-Fermi density of both of the atoms can be determined by

$$n\left(r\right) = \frac{2^{3/2}}{3\pi^2}\left(\mu - \frac{Z}{r}\right)^{3/2} \quad \text{for} \quad \mu \geq \frac{Z}{r} \tag{1.1}$$

with $n(r) = 0$ for $\mu < Z/r$ and where μ is a fixed chemical potential for each of the atoms [1]. This indicates that each of the atom's density will have a similar general structure relative to its chemical potential and, as a result, its energy since the chemical potential provides the same value as the ionization energy for an atom. Even so, there remains a sharp distinctness in understanding the energy of each of these atoms. By Virial theorem in classical mechanics that applies for the atom's $-Z/r$ potential [8], we have a simple relation for the kinetic energy, T, and nuclear potential energy, U, for the non-interacting atom,

$$2T = -U \tag{1.2}$$

However, for the real atom, there exists a potential term for the electron-electron interaction in the system, U_{ee},

$$2T = -U_{ee} - U \tag{1.3}$$

Through this paper, we will examine the filling of the shells, the energy, chemical potential, ionization energy, and the density of the non-interacting atom and accordingly speculate as to what particular information can be translated to the real case. We will expand upon Englert's semiclassical theory for the non-interacting atom [9] to examine the filling of the shells, the energy, chemical potential, and ionization energy of the non-interacting atom similar to the manner in which Schwinger studied the real atom using semiclassics [10]. Also, a model for the density of the non-interacting atom will be obtained primarily by modeling the quantum correction that might be approximated using semiclassical methods in Kohn-Sham GF theory at some future time. At present, there is no formal derivation of those corrections. Regardless as to whether any of our understanding of the non-interacting atom can be directly translated to the real atom, if Kohn-Sham GF theory is developed for the non-interacting case to coincide with our results, then similar theory can be applied to understand the real case.

1.2 Introductory Theory

Using a relatively simple but novel approach with semiclassics, Englert derives the following expression for the binding energy of a doubly occupied atom with non-interacting

electrons, $-E$,

$$-E = Z^2 \left(y - \frac{1}{2} + \varphi(y) \right) \tag{1.4}$$

where

$$y^3 - \frac{1}{4}y = \frac{3}{2}N, \tag{1.5}$$

$$\langle y \rangle = y - \left\lfloor y + \frac{1}{2} \right\rfloor \tag{1.6}$$

and

$$\varphi(y) := \left(\langle y \rangle^2 - \frac{1}{4} \right) \frac{y - \frac{2}{3} \langle y \rangle}{(y - \langle y \rangle)^2} \tag{1.7}$$

with $\lfloor x \rfloor$ denoting the greatest integer less than x [9]. This Coloumb energy is a continuous function of y, however it is not continuously differentiable due to cusps where the valence shell is filled, e.g. $N = 2, 10, 28, 60, \ldots$. This representation for $-E$ has a very similar structure to a direct calculation by summing up the energy of each shell,

$$-E = \sum_{n=1}^{M-1} \sum_{l=0}^{n-1} \frac{Z^2}{n^2} (2l+1) + E_{val} = Z^2(M-1) + E_{val} \tag{1.8}$$

where Mth shell is the valence shell, which has an energy $-E_{val}$.

By fixing a finite chemical potential $\mu = -Z/r_F$ that is satisfied at a distance r_F, we can obtain a particular Thomas-Fermi density for the non-interacting atom from Eq.(1.1) for $0 \leq r \leq r_F$,

$$n_Z^{TF}(r) = \frac{(2Z)^{3/2}}{3\pi^2} \left(\frac{1}{r} - \frac{1}{r_F} \right)^{3/2} \tag{1.9}$$

with $n_Z^{TF} = 0$ for $r > r_F$. From here, the fixed distance r_F can be determined to satisfy the normalization condition of the density,

$$r_F = 2^{1/3} 3^{2/3} Z^{-1/3} \tag{1.10}$$

However, before working with this Thomas-Fermi density and other functions at the atomic level, let us scale the atom appropriately. Since the atom has a size of $Z^{-1/3}$ as shown by Eq.(1.10), let us introduce a new variable $x = Z^{1/3}r$ so that $x_F = 2^{1/3} 3^{2/3} = Z^{1/3} r_F$ and $Z^2 n(x) = \tilde{n}(r)$. For the finite Thomas-Fermi case, we have

$$n^{TF}(x) = \frac{2^{3/2}}{3\pi^2} \left(\frac{1}{x} - \frac{1}{x_F} \right)^{3/2}. \tag{1.11}$$

with $n^{TF}(x) = 0$ elsewhere. Thus the approximate radius of any finite non-interacting atom is then x_F using our new scaling. Likewise, we can scale the radial densities,

$$4\pi Z^{4/3} x^2 n(x) = 4\pi r^2 \tilde{n}(r). \tag{1.12}$$

3

From here, all atomic densities will assume this scaling, including the exact density for a non-interacting atom with M fully-occupied shells, which can be computing using a sum of radial functions [4],

$$n(x) = 2 \sum_{k=1}^{M} \sum_{l=0}^{k-1} \frac{1}{4\pi} (2l+1) |R_{k,l}(x)|^2 \tag{1.13}$$

where

$$R_{k,l}(x) = Z \sqrt{\left(\frac{2}{k}\right)^3 \frac{(k-l-1)!}{2k(k+l)!}} e^{-\rho/2} \rho^l L_{k-l-1}^{2l+1}(\rho) \tag{1.14}$$

$$\rho = \frac{2Z^{2/3}}{k} x \tag{1.15}$$

and L_n^m are associated Laguerre polynomials.
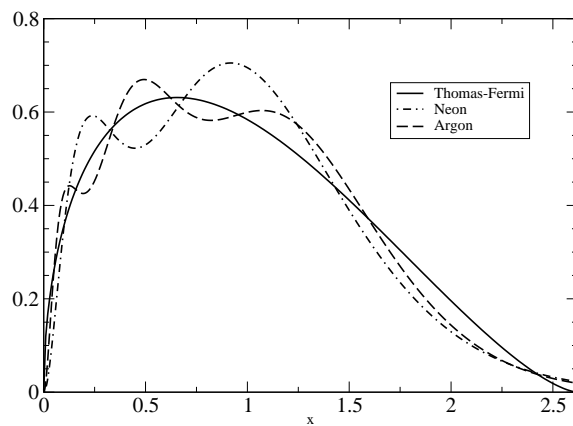
Figure 1.1: The exact Radial densities of non-interacting Neon and Argon plotted with the Thomas-Fermi approximation, $n^{TF}(x)$, on the scale $x = Z^{1/3}r$

4

Chapter 2

Theory and Illustration

2.1 Expanding $y(N)$ and φ

Englert approximates the value of y as it appears in Eq.(1.5) as a function of N using the series

$$y(N) = \left(\frac{3}{2}N\right)^{1/3} + \frac{1}{12}\left(\frac{3}{2}N\right)^{-1/3} + \cdots \tag{2.1}$$

with the following terms alternating in sign. However, the exact value of y as a function of N can be solved from Cardan's cubic formula,

$$y(N) = \left(\frac{3}{4}N\right)^{1/3}\left[\left(1+\sqrt{1-\frac{1}{972N^2}}\right)^{1/3} + \left(1-\sqrt{1-\frac{1}{972N^2}}\right)^{1/3}\right]. \tag{2.2}$$

Computing a Taylor series for this solution, we have the following series expansion for $y(N)$,

$$y(N) = \sum_{k=0}^{\infty} a_k \left(\frac{3}{2}N\right)^{p_k} \tag{2.3}$$

with $p_k = 1/2 - k - (-1/6)^k$ for $k = 0, 1, 2, \ldots$ and the first few constants of $\{a_k\}$ provided in the Appendix with a_0 and a_1 consistent with Englert's first two terms provided by Eq.(2.1).

It is key to note that $y - \frac{1}{2}$ gives the value of how many shells of the atom have been filled for a given N, which could even be a fractional particle number. So, the $\lfloor y + \frac{1}{2} \rfloor$th shell is the valence shell, $\lfloor y - \frac{1}{2} \rfloor$ shells have been filled, and $y(N)$ provides a continuous form in which the shells of the non-interacting atom fill as electrons are added. Once again, the shells of the real atom do not fill in this fashion since the non-interacting atom has its own, distinct periodic table.

From here, let us translate how the shells fill as more electrons are added to the non-interacting to how the shells fill in one particular non-interacting atom as the distance from the nucleus, x, varies. Suppose a sphere of radius x is placed around the nucleus of a non-interacting atom. We consider the atomic matter within the sphere as an ion in its own right due to the fact there is no electron-electron repulsion and Coloumb energy

is the only energy in this bounded system. Instead of having N electrons in its orbit, our new atom has $N \int_0^x n(x') d^3x'$ electrons where $n(x)$ is the density of the actual non-interacting atom on a $Z^{-1/3}$ scale. From here, we can arrive to an expression analogous to Eq.(1.5) that assigns a value of y for this ion within a radius x and also an expression for its energy,

$$y^3(x) - \frac{1}{4}y(x) = \frac{3}{2}N \int_0^x n(x') d^3x' \tag{2.4}$$

$$-E(x) = Z^2 \left(y(x) - \frac{1}{2} + \varphi(y(x)) \right). \tag{2.5}$$

This implicit function $y(x)$, then, provides how many shells have been filled a distance x from the nucleus, $\lfloor y(x) + 1/2 \rfloor$. Using Eq.(2.3), $y(x)$ can be written as an explicit series expansion in terms of x alone.

Englert derives an expansion for the oscillation term of the energy, φ, and, in turn, a dominant piece of φ which is highly accurate for large y [9].

$$\varphi(y) = \left(\langle y \rangle^2 - \frac{1}{4} \right) \left(\frac{1}{y} \sum_{k=0}^{\infty} \frac{k+3}{3} \left(\frac{\langle y \rangle}{y} \right)^k \right) \tag{2.6}$$

$$\varphi(y) = \left(\langle y \rangle^2 - \frac{1}{4} \right) \left(\frac{1}{y} + \cdots \right). \tag{2.7}$$

φ itself may not be periodic, however it does have an element of periodicity in $\langle y \rangle$, which allows us to further expand φ using Fourier series. This brings us to the following smooth expansion of φ,

$$\varphi(y) = \left(-\frac{1}{6} + \sum_{n=0}^{\infty} \frac{(-1)^n}{n^2 \pi^2} \cos(2n\pi y) \right) \cdot \left(\sum_{k=0}^{\infty} \frac{k+3}{3} \frac{1}{y^{k+1}} \left(\sum_{n\pi} \sin(2n\pi y) \right)^k \right)$$

with a dominant piece,

$$\left(-\frac{1}{6} + \sum_{n=0}^{\infty} \frac{(-1)^n}{n^2 \pi^2} \cos(2n\pi y) \right) \left(\frac{1}{y} + \cdots \right). \tag{2.8}$$

From here, the oscillation of the energy as it depends on y can be "denoised" by truncating all or only high frequency oscillations, so that the energy has little oscillation as the shells are filled. In turn, this essentially approximates the energy of the atom without the quantum shell-structure and may very well correspond to energy obtained using a Thomas-Fermi approximation, but we will not explore this possibility.

2.2 An Upper Bound for $-E$

Now, with an expression for y in terms of N, let us derive an upper bound for $-E$ in terms of Z for the neutral case $N = Z$. Note that the periodic term $\langle y \rangle$ as provided in Eq.(1.6) ranges in the interval $\left[-\frac{1}{2}, \frac{1}{2} \right)$ and, as a result, that φ is nonpositive,

$$\varphi(y) = \left(\langle y \rangle^2 - \frac{1}{4} \right) \frac{y - \frac{2}{3}\langle y \rangle}{(y - \langle y \rangle)^2} \le 0. \tag{2.9}$$
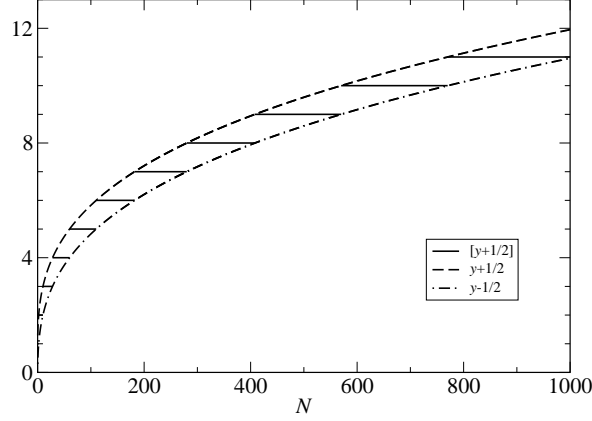
Figure 2.1: The number of filled shells in a non-interacting atom, $\lfloor y(N) + 1/2 \rfloor$, as it depends on the number of electrons in orbit, N, compared with the smooth approximations $y(N) + 1/2$ and $y(N) - 1/2$.

When the shells are doubly occupied, $\langle y \rangle$ attains a value of $-\frac{1}{2}$ and, thus, we have that $\varphi(y) \equiv 0$ and

$$-E \geq Z^2 \left(y - \frac{1}{2} \right). \tag{2.10}$$

by the non-positivity of φ. This expression is essentially the same as the energy provided by Eq.(1.8) with $E_{val} = 0$ and $M - 1 = y - \frac{1}{2}$. Now, applying our series for $y(N)$ in Eq.(2.3), the binding energy for this case can be written as

$$-E \geq Z^2 \left(\sum_{k=0}^{\infty} a_k \left(\frac{3}{2} N \right)^{p_k} - \frac{1}{2} \right). \tag{2.11}$$

If we consider the neutral case when $N = Z$, then E can be written in terms of Z alone, and we have the following sharp upper bound, $-E_U$, for $-E$,

$$-E_U(Z) = \sum_{k=0}^{\infty} a_k \left(\frac{3}{2} Z \right)^{p_k+2} - \frac{1}{2} Z^2. \tag{2.12}$$

2.3 A Lower Bound for $-E$

In order to derive a lower bound for $-E$, we will minimize the oscillation term φ. Substituting $y - \lfloor y + \frac{1}{2} \rfloor$ for $\langle y \rangle$, we can expand φ as so,

$$\varphi(y) = \frac{1}{3 \lfloor y + \frac{1}{2} \rfloor^2} y^3 - \left(1 + \frac{1}{12 \lfloor y + \frac{1}{2} \rfloor^2} \right) y - \frac{1}{6 \lfloor y + \frac{1}{2} \rfloor} + \frac{2}{3} \lfloor y + \frac{1}{2} \rfloor. \tag{2.13}$$

Now, fix y, and let $k = \lfloor y + \frac{1}{2} \rfloor$ become its own independent variable. Let us further generalize φ for this fixed y by defining the following multivariable function for $k \in [-\frac{1}{2}, \frac{1}{2})$ and $y \geq 0$,

$$\varphi^*(y, k) = \frac{1}{k^2} \left(\frac{y^3}{3} - \frac{y}{12} \right) - \frac{1}{6k} + \frac{2}{3} k - y. \tag{2.14}$$

7

From here, we can find a lower bound for φ by determining the minimum value that φ^* can attain among all k for any given y. This can be done by differentiating φ^* with respect to k and equating the expression to zero and then solving for a particular $\tilde{k}$ in terms of y. This critical value $\tilde{k}$ must globally minimize φ^* since $\partial^2 \varphi^*/\partial y^2 \geq 0$ for k and y in our domain.

$$\frac{\partial \varphi^*}{\partial k}\left(y, \tilde{k}\right) = 0 = -\frac{2}{\tilde{k}^3}\left(\frac{y^3}{3} - \frac{y}{12}\right) + \frac{1}{6\tilde{k}^2} + \frac{2}{3} \tag{2.15}$$

$$0 = \tilde{k}^3 + \frac{1}{4}\tilde{k} - y^3 + \frac{y}{4} \tag{2.16}$$

From here, we can once again use Cardan's cubic formula to solve for $\tilde{k}$ in terms of y, but this would provide a very convoluted expression due to the cubic and linear terms of y. As an alternative, guess $\tilde{k} = y$ as a leading term for the solution to Eq.(2.16) and then iteratively solve for the succeeding terms based on resultant error terms. Hence, the following expansion for our critical value, $\tilde{k}$,

$$k = \sum_{k=0}^{\infty} b_k y^{1-2k}. \tag{2.17}$$

After computing $\tilde{k}^{-2}$ and $\tilde{k}^{-1}$ from Eq.(2.17), we can input this critical value of k into φ^* and obtain a lower bound for φ and, as a result, a lower bound for $-E$ in terms of y is reached. Again, we can use the series expansion of y in terms of N with series expansion for powers of y that can be derived from our expansion of $y(N)$, and let $N = Z$.

$$\varphi \geq \sum_{k=1}^{\infty} c_k y^{1-2k} \tag{2.18}$$

$$-E \geq Z^2 \left(y - \frac{1}{2}\sum_{k=1}^{\infty} c_k y^{1-2k} \right) \tag{2.19}$$

$$-E \geq Z^2 \sum_{k=0}^{\infty} d_k N^{q_k}. \tag{2.20}$$

where $q_k = (1 - 2k)/3$. This brings us to a sharp lower bound for $-E$ in terms of N alone, $-E_L(N)$, to accompany $-E_U(N)$,

$$-E_L(N) = \sum_{k=0}^{\infty} d_k Z^{q_k+2} \tag{2.21}$$

Note that the first two terms of the upper and lower bounds coincide with one another while the range of oscillation of $-E$ grows like $Z^{5/3} \sim Z^2 y^{-1}$, which can be understood as the difference between the upper and lower bounds or the range in which φ oscillates. This oscillation of the energy occurs at a higher power of Z than it does for the real atom, which is at $Z^{4/3}$ [11].
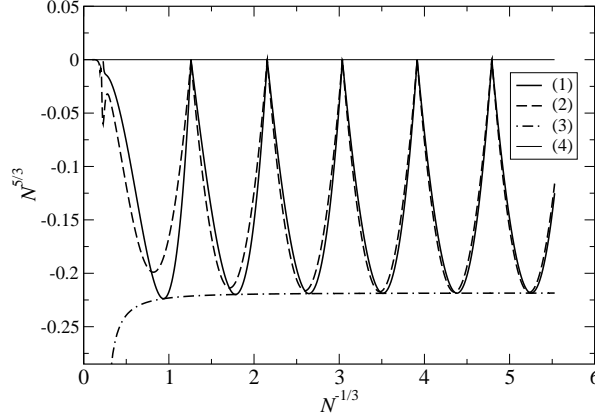
Figure 2.2: (1) is $-E_U - (-E)$. (2) is the dominant piece of φ as provided in Eq.(2.7). (3) is $-E_U - (-E_L)$. (4) is a zero line.

2.4 An Exact Energy Density

Now that we have studied how the energy of the non-interacting atom depends on the particle number, let us examine the energy of just particular non-interacting atom. Differentiating the energy of a particular non-interacting atom within a radius x, $-E(x)$ in Eq.(2.5) with respect to x, we have

$$-\frac{dE}{dx} = Z^2 \left(1 + \frac{d\varphi}{dy}\right) \frac{dy}{dx}. \tag{2.22}$$

We can determine dy/dx by differentiating Eq.(2.4) implicitly and find $d\varphi/dy$ by differentiating Eq.(1.7) and, from here, come to a simple expression for $-dE/dx$, the energy density of the atom,

$$\frac{dy}{dx} = \frac{4\pi x^2 N n(x)}{2y^2(x) - \frac{1}{6}} \tag{2.23}$$

$$\frac{d\varphi}{dy} = \frac{1}{\left\lfloor y(x) + \frac{1}{2} \right\rfloor^2} \left(y^2(x) - \frac{1}{12}\right) - 1 \tag{2.24}$$

$$-\frac{dE}{dx} = \frac{1}{2} N Z^2 \frac{4\pi x^2 n(x)}{\left\lfloor y(x) + \frac{1}{2} \right\rfloor^2}. \tag{2.25}$$

Integrating both sides, then, provides an exact density functional for the energy of the entire atom,

$$-E[n] = \frac{1}{2} N Z^2 \int \frac{n(x)}{\left\lfloor y(x) + \frac{1}{2} \right\rfloor^2} d^3x. \tag{2.26}$$

Within this functional, we see a resemblance to the first expression for $-E$ in Eq.(1.8). The value of n in Eq.(1.8) designates which shell is being filled, which is essentially the
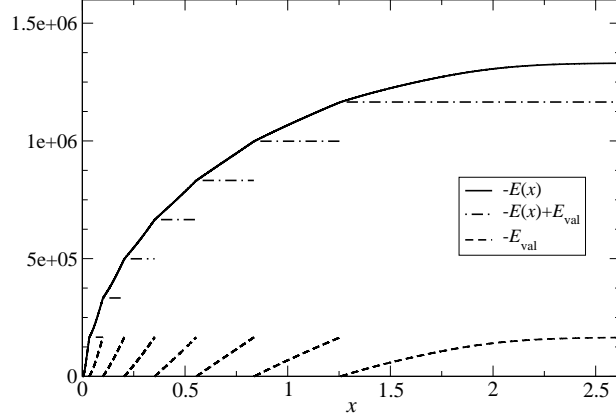
Figure 2.3: $-E(x)$ plotted along with $-E(x) + E_{val}$ and E_{val}.

same as $\lfloor y(x) + \frac{1}{2} \rfloor$, while summing $2l + 1$ and integrating $Nn(x)$ each provide the filling of these shells with electrons for their respective computations.

Using the Euler-Lagrange equation, we have that the universal function, $F[n]$, which provides a value for the kinetic energy and energy by electron-electron interaction of the atom, can be expressed as follows,

$$F[n] = \int \left(\frac{Z^{4/3}}{x} - \frac{NZ^2}{\lfloor y(x) + 1/2 \rfloor} \right) n(x) d^3x. \tag{2.27}$$

Now, since we are working in particular with a non-interacting atom, there is no electron-electron interaction, which indicates that this is a functional that provides the kinetic energy. This functional is particularly interesting to compare to the Thomas-Fermi kinetic energy functional,

$$T_0[n] = A_s \int n^{5/3}(x) d^3x \tag{2.28}$$

to test its accuracy on this simple non-interacting system.

2.5 Examining Chemical Potential & Ionization Energy

Using $\mu = -Z/r_F$ as the fixed chemical potential of the atom from Eq.(1.10), we can approximate the chemical potential as follows,

$$\mu = \alpha_0 Z^{4/3}. \tag{2.29}$$

where $\alpha_0 = -(2^{1/3}3^{2/3})^{-1}$. For this non-interacting atom, the ionization energy and the chemical potential should be the same quantity, so, let us study the ionization energy as means to determine the accuracy of the Thomas-Fermi approximation for the chemical potential.

The ionization for the kth shell of this atom can be written as

$$\epsilon_k = -\frac{Z^2}{2k^2}. \tag{2.30}$$

Now, if we use the sharp inequality $y(\tilde{N}) - \frac{1}{2} \le k = \lfloor y(\tilde{N}) + \frac{1}{2} \rfloor \le y(\tilde{N}) + \frac{1}{2}$ where $\tilde{N}$ is the number of electrons within the first k shells, we can construct the following lower and upper bounds for the ionization energy, ϵ_k^U and ϵ_k^L respectively, with the magnitude of the lower bound being greater due to the negativity of ϵ_k,

$$\epsilon_k^L = -\frac{Z^2}{2\left(y(\tilde{N}) - \frac{1}{2}\right)^2} = Z^2 \sum_{j=0}^{\infty} \alpha_j \tilde{N}^{s_j} \tag{2.31}$$

$$\epsilon_k^U = -\frac{Z^2}{2\left(y(\tilde{N}) + \frac{1}{2}\right)^2} = Z^2 \sum_{j=0}^{\infty} (-1)^j \alpha_j \tilde{N}^{s_j}. \tag{2.32}$$

where $s_j = (-2 - j)/3$ for $j = 0, 1, 2, \dots$. Specifically for the valence Mth shell, we have for the neutral case,

$$\epsilon_M^L = \sum_{j=0}^{\infty} \alpha_j Z^{s_j + 2} \tag{2.33}$$

$$\epsilon_M^U = \sum_{j=0}^{\infty} (-1)^j \alpha_j Z^{s_j + 2} \tag{2.34}$$

with the first term $\alpha_0 Z^{4/3}$ of each bound agreeing with the value of the Thomas-Fermi chemical potential in Eq.(2.29). Note that both bounds for the ionization energy and Thomas-Fermi approximation for the chemical potential differ by a linear term with respect to Z.

The leading term of the ionization energy can be reached using the energy of the non-interacting atom. Taking the difference in energies when only one electron is removed with a constant $-Z/r$ potential, we have,

$$E(Z, N) - E(Z, N - 1) = \alpha_0 N^{4/3} + \dots \tag{2.35}$$

Computing the functional derivative of the density functional in Eq.(2.26) also obtains the exact chemical potential as a step function,

$$\frac{\delta E}{\delta n} = -\frac{Z^2}{2\lfloor y(x) + \frac{1}{2} \rfloor^2} = \epsilon_{\lfloor y(x) + \frac{1}{2} \rfloor} \tag{2.36}$$

which in fact confirms that our density functional is in fact correct.

Chapter 3

Modeling Densities

3.1 Regions and Convergence of the Non-Interacting Densities

As means to understand the non-interacting densities, let us model the exact densities as a sequence of functions. Consider the sequence of functions $\{n_M\}$, where $n_M(x)$ is the density of a neutral non-interacting atom with M full, doubly occupied shells. Only the index M will be used since Z can be determined by Eq.(1.5) with $y(Z) = M + 1/2$, and so as $Z \to \infty$, it follows that $M \to \infty$. Then, let $\{n_M^{mod}(x)\}$ be the corresponding sequence of functions we will construct that model the exact sequence $\{n_M(x)\}$.

Lieb approached the real atom by dividing it into five regions in which the density takes different forms [2]. We will begin to examine the density of the non-interacting atom in a similar fashion by defining three regions on our $Z^{-1/3}$ scale in which the density takes different form: the inner region, $[0, \beta]$; the intermediate region $(\beta, \eta]$; and the outer region, (η, ∞) where

$$\beta = 0.4632 Z^{-2/3} \quad \text{and} \quad \eta = \left(\frac{1}{x_F} + 0.512993 Z^{-0.23058} + 0.590131 Z^{-0.558412} \right)^{-1}. \quad (3.1)$$

β is an approximation of the first nonzero intersection point of the Thomas-Fermi density, $n^{TF}(x)$, and the exact density, $n(x)$, while η is the second to last intersection point. The beginning of the outer region, η does not scale nicely with the nucleus as the beginning of the intermediate region, β, does, but instead the value of the Thomas-Fermi density at that distance away, $n^{TF}(\eta)$, scales as a polynomial of Z. The inner region collapses as $Z \to \infty$ and, also, we have that the outer region vanishes since $Z^{-1/3} x_F = r_F \to \infty$ as $Z \to \infty$. This indicates that the intermediate region should dominate as the atom becomes large.

The non-interacting densities scale differently through each region, so different functions will be used for each region by constructing $\{n_M^{mod}\}$ in a piecewise format. There may exist more than three regions in which the non-interacting atom scales differently, but for modeling purposes, we will only consider these three. The inner and outer regions will be constructed in a direct fashion while modeling the intermediate region will be guided by Heilmann and Lieb's hydrogenic density [12], ρ^H, which is is the limit function
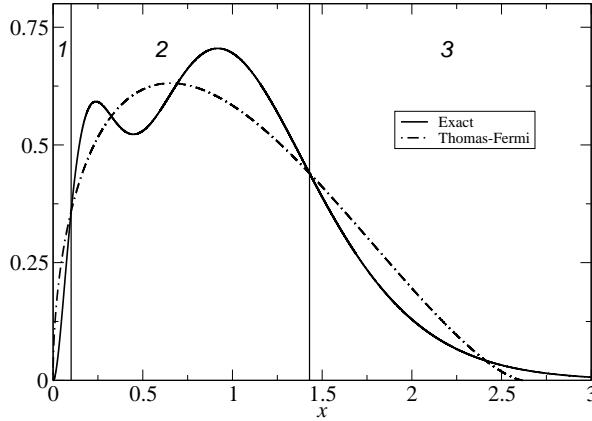
Figure 3.1: The inner, intermediate, and outer regions of the radial density of non-interacting Helium labeled by 1, 2, and 3, respectively.

for the densities of these non-interacting atoms as $Z \to \infty$,

$$\rho^H(r) = \frac{\sqrt{2}}{\pi^2} r^{-3/2} \left[\sum_{j=0}^{\infty} a_j (8r)^{-j} - \sin(\sqrt{32r}) \sum_{j=1}^{\infty} b_j (8r)^{-j} \right.$$
$$\left. + \cos(\sqrt{32r}) \sum_{j=1}^{\infty} c_j (8r)^{-j-1/2} \right] \tag{3.2}$$

on a scale length of Z^{-1} with respect to r and typical amplictude Z^3. The infinite scaled Thomas-Fermi function asymptotic to the hydrogenic density on this scaling is $\rho^{TF}(x) = 2^{3/2}(3\pi^2)^{-1} x^{-3/2}$, which remains consistent with Eq.(1.5) as $Z \to \infty$. It would likely be difficult to study the convergence of the finite densities to the hydrogenic densities since the Thomas-Fermi densities for the finite and infinite case are different and the Thomas-Fermi density becomes exact as $Z \to \infty$ [2]. So, let us examine how the difference between non-interacting densities and Burke's finite Thomas-Fermi density converge to the difference between the hydrogenic density and its respective Thomas-Fermi density. Define the sequence of functions $\{\xi_Z\}$ by

$$\xi_M(x) := \left[n_M(Z^{-2/3}x) - n^{TF}(Z^{-2/3}x) \right] Z^{1/3} \tag{3.3}$$

which uniformly converge to the limit function

$$\xi_\infty(x) := \rho^H(x) - \frac{2^{3/2}}{3\pi^2} x^{-3/2} \tag{3.4}$$

as $Z \to \infty$ on the intermediate region. Essentially, this sequence of functions, $\{\xi_M\}$, is just the scaled quantum correction to the Thomas-Fermi density. Thus, to obtain the a model for $\{n_M(x)\}$, a model for $\{\xi_Z\}$ will be constructed and then added to the Thomas-Fermi density on the intermediate region. These functions scale like Z^{-1} due to a strong resemblance of shell location in the quantum correction on this scale for different non-interacting atoms as demonstrated in Fig.(3.2). It is important to note that on this Z^{-1} scaling, the inner region does not collapse but remains at a constant size since $\beta \sim Z^{-2/3}$ on a $Z^{-1/3}$ scale while the intermediate region dominates the remainder of the domain as Z becomes large.

13
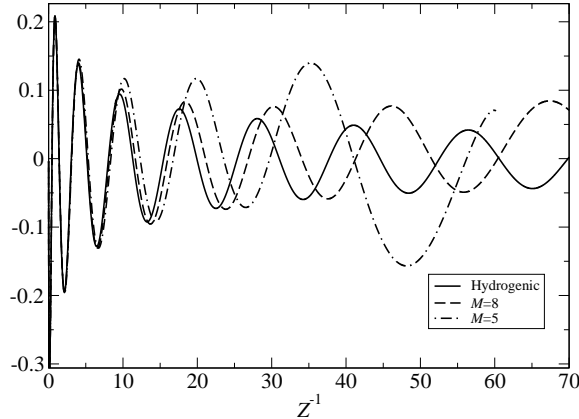
Figure 3.2: $4\pi x^2 \xi_5(x)$ and $4\pi x^2 \xi_8(x)$ plotted on their respective inner and intermediate regions along with their limit function $4\pi x^2 \xi_\infty(x)$ on a Z^{-1} length scale. A strong similarity is shown as $x \to 0$.

3.2 Modeling the Inner Region

Since the external potential dominates the Schrödinger equation for distances near the nucleus, Kato's Cusp Condition holds for small δ [13],

$$\frac{dn}{dx}\Big|_{x=\delta} = -2Z^{2/3}n(\delta). \tag{3.5}$$

Provided with the initial condition $n(0) = 2Z^3/\pi$ as computed using Eq.(1.13), we now can solve this simple first order linear homogeneous initial value problem to obtain the following exponential function,

$$n(\delta) = \frac{2Z}{\pi} \sum_{k=1}^{M} \frac{1}{k^3} \exp(-2Z^{2/3}\delta) \tag{3.6}$$

This exponential function actually serves as a highly accurate approximation for the exact density on the entire inner region, so we can define

$$n_M^{mod}(x) = \frac{2Z}{\pi} \sum_{k=1}^{M} \frac{1}{k^3} \exp(-2Z^{2/3}x) \tag{3.7}$$

for $x \in [0.\beta]$.

Since β is an intersection point between the exact and Thomas-Fermi densities, it would be ideal for the condition

$$\lim_{x \to \beta^-} \left[n_M^{mod}(x) - n^{TF}(x) \right] = 0 \tag{3.8}$$

to be met. However, based off of this exponential construction, this is not the case, though this limit is very small due to the high accuracy of the estimation.

This very same exponential function can be obtained simply by the dominant term in the normalized sum of radial functions given by Eq.(1.13) as $x \to 0$, which is the first radial function multiplied by a sum of the inverse cubes of each shell number, $2\sum_{k=1}^{M}(1/k^3)|R_{1,0}|^2$.

14
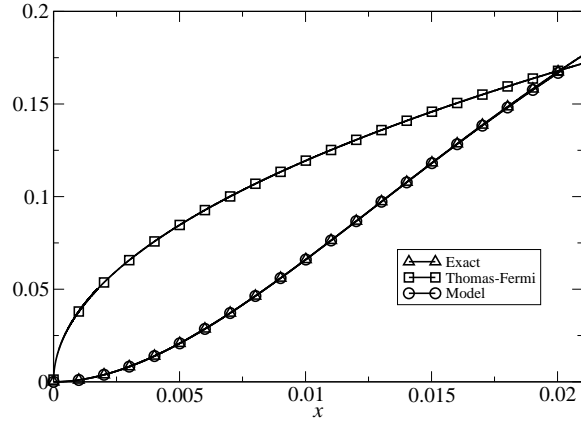
Figure 3.3: $4\pi x^2 n_5^{mod}(x)$ plotted in the inner region as a model for $4\pi x^2 n_5(x)$ as an improvement over the Thomas-Fermi approximation.
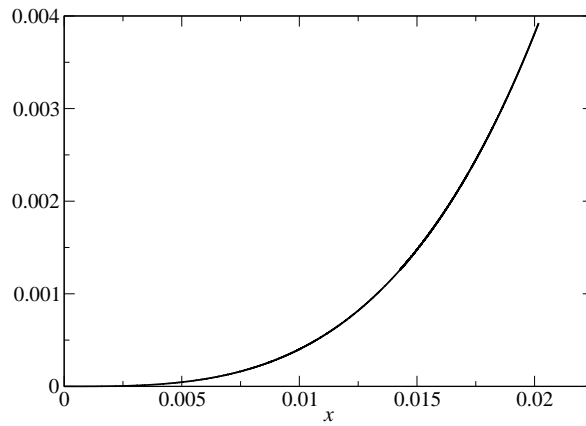
Figure 3.4: The relative difference $1 - n_5^{mod}(x)/n_5(x)$ in the inner region.

3.3 Modeling the Intermediate Region

Let us now model the density of the intermediate region of the atom such that when scaled appropriately, it roughly approaches Heilmann and Lieb's hydrogenic density, ρ^H in Eq.(3.2), as $Z \to \infty$. So, let us implement the same structure as ρ^H in our model as so for $x \in (\beta, \eta]$,

$$n_M^{mod}(x) = n^{TF}(x) + Z^{-1/3} A(x; Z) \sin \left[Z^{1/3} \theta(x) - l(x; \beta; \eta) \right] + Z^{1/3} S(x) \tag{3.9}$$

where

$$A(x; Z) = \frac{3}{8\sqrt{2}\pi^2} x^{-5/2} \exp(k_1 x^2 - k_2 Z^{-2/3} x^{-1}) \tag{3.10}$$

$$\theta(x) = 2\pi \left(\frac{3}{2} \int_0^x n^{TF}(x') d^3 x' \right)^{1/3} + 6\pi \left(1 - \left(\frac{\pi^2}{6} \right)^{1/3} \right) x^2 n^{TF}(x) \tag{3.11}$$

$$S(x) = \frac{1}{32} x^{-2} \frac{d}{dx} \left(x^2 n^{TF}(x) \right) + k_3 n^{TF}(x) + k_4 x^{-2} \int_0^x n^{TF}(x') d^3 x' \tag{3.12}$$

$$l(x) = \left(\theta(\eta) + \frac{S(\eta)}{A(\eta; Z)} - 2M\pi \right) \frac{(x - \beta)}{(\eta - \beta)} + \left(\theta(\beta) + \frac{S(\beta)}{A(\beta; Z)} - \pi \right) \frac{(x - \eta)}{(\beta - \eta)} \tag{3.13}$$

with $k_1 = 1/3, k_2 = 2/5, k_3 = 0.0013, k_4 = 0.0143239$ as roughly estimated coefficients. The hydrogenic density closely reflects the exact finite densities as $x \to \beta \to 0$, so as $x \to \beta \to 0$, we appropriately have

$$n_M^{mod}(Z^{-2/3} x) \to \frac{\sqrt{2}}{\pi^2} r^{-3/2} \left[(a_0 + a_1)(8r)^{-j} - \sin(\sqrt{32r}) b_1 (8r)^{-j} \right] \tag{3.14}$$

with constants provided by those in the hydrogenic density. The fact that the dominant pieces of $n_M^{mod}(Z^{-2/3} x)$ only approach the dominant pieces of the hydrogenic density, we have that the sequence $\{\xi_M\}$ does not actually converge to $\{\xi_\infty\}$ but only provides a sense of 'near convergence'. Only this near convergence is achieved for the sake of relative simplicity of our model to only consider dominant pieces.

Both of $A(x; Z)$ and $S(x)$ are constructed based off of the structure of their respective parts in the hydrogenic density and adjusted just to fit the sequence of functions $\{\xi_M\}$ appropriately. The amplitude, $A(x; Z)$, uses the dominant $x^{-5/2}$ piece along with an exponential factor which approaches 1 as $x \to 0$. The adjustments for $S(x)$ do not scale with Z, which indicates that there is likely one unique function in the exact quantum correction that applies for any M. All analytic constants for these two functions are determined so that we have this element of 'near convergence' to ρ^H while numerical constants are simply chosen for an appeared higher achieved accuracy.

The frequency of the oscillation, $\theta(x)$, is first motivated by the continuous form of Englert's rate in which the electrons fill the shells, $y(x)$, as provided by Eq.(2.4), which should give some basic form to the manner in which the shells appear as oscillations in

each $\{\xi_M\}$. As $x \to 0$, we have a major piece of $\theta(x)$ within an amproximation for $y(x)$ as the frequency,

$$y(x) \to \left(\frac{3}{2} Z \int_0^x n^{TF}(x') d^3 x'\right)^{1/3} \tag{3.15}$$

Only the dominant term of $y(x)$ is used so that $\theta(x)$ can accurately scale like $Z^{1/3}$ since the remainder of a series expansion does not actually do so, which is evident in Eq.(2.3). The appropriate adjustment to this estimation for the frequency is contributed by the Thomas-Fermi radial density since it appears as though the actual shape of the density that contributes to the offset of the shell oscillations in each $\{\xi_M\}$ spawns from the actual filling of shells in $y(x)$. Once again, analytic coefficients are determined for 'near convergence' so that $\theta(x) \to \sqrt{32x}$. Like $S(x)$, $\theta(x)$ does not scale with Z, and indicates that there is likely one unique function for the angular frequency in the exact quantum correction that applies for any M.

The alter in phase of the oscillation provided by $l(x; \beta; \eta)$ is a Lagrange interpolation line constructed under the conditions

$$\lim_{x \to \beta^+} \left[n_M^{mod}(x) - n^{TF}(x)\right] = 0 \quad \text{and} \quad \lim_{x \to \eta^-} \left[n_M^{mod}(x) - n^{TF}(x)\right] = 0 \tag{3.16}$$

set by the notion that β and η are intersection points of the exact and Thomas-Fermi densities. Since the condition set by Eq.(3.8) is nearly met, we then do not have n_M^{mod} continuous at β though we do have a sense of 'near continuity' due to the high accuracy of approximation in the inner region.

The estimated frequency $\theta(x) + l(x; \eta; \beta)$, though quite accurate, is only an estimate, so as M grows, the approximation for the frequency differs from that of the exact frequency of $\{\xi_M\}$ and the two can become completely out of phase for a given distance away from the nucleus. So, an approximation for the bound of the error in the intermediate region for a given x^* can be as large as $2A(x^*; Z)$, which is quite poor.
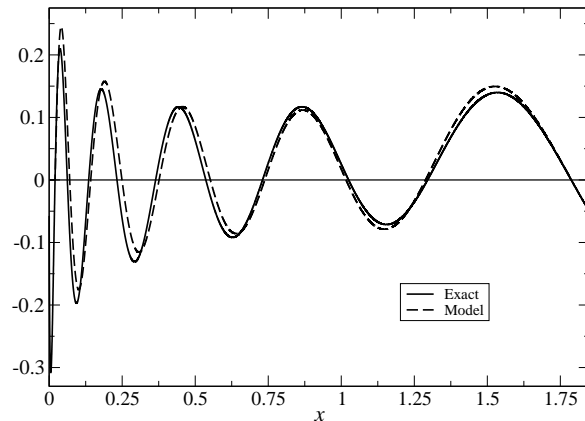
Figure 3.5: $4\pi x^2 \left(n_5^{mod}(Z^{-2/3}x) - n^{TF}(Z^{-2/3}x)\right) Z^{1/3}$ plotted in the intermediate region as a model for $4\pi x^2 \xi_5(x)$.

3.4 Modeling the Outer Region

Let us begin to examine the non-interacting density in the outer region through an understanding of the radial functions for the outer shell provided in Eq.(1.13) as $Z \to \infty$.

$$2 \sum_{l=0}^{M-1} \frac{1}{4\pi} (2l+1)|R_{M,l}(\rho)|^2 \quad \to \quad \frac{1}{2\pi} |R_{M,0}|^2 \tag{3.17}$$

$$\to \quad \frac{2Z^3}{\pi M^6} e^{-\rho} \left(L_{M-1}^1(\rho) \right)^2 \tag{3.18}$$

$$\to \quad \frac{2^{2M-1} Z^{4M/3}}{\pi M^{2M+3}((M-1)!)^2} x^{2(M-1)} \exp\left(-\frac{2}{M} Z^{2/3} x \right) \tag{3.19}$$

We can also arrive to this asymptotic function using other quantum mechanical methods. When deviating far from the nucleus, the N-electron ground state wavefunction of any atom collapses to the product of the square root of the density and the $(N-1)$-electron ground state wave function. This results in a certain differential equation resembling the Schrödinger equation that is solved by

$$\sqrt{n(x)} \to A \left(Z^{-1/3} x \right)^\beta \exp\left(-\alpha Z^{-1/3} x \right) \tag{3.20}$$

where $\alpha = \sqrt{2I}$, $\beta = Z/\alpha - 1$, and I is the first ionization potential [14][15]. The first ionization energy as explored in Section 2.5 can be written as $I = -\epsilon_M = Z^2/(2M^2)$, which indicates that $\alpha = Z/M$ and $\beta = M - 1$. This indicates that the expression in Eq.(3.19) provided by radial functions then satisfies the condition in Eq.(3.20) with the amplitude, A, scaling with both Z and M.

Using the structure of the expression in Eq.(3.19), we can construct a model for the non-interacting density in the outer region by adding a second term within the exponential function determined numerically,

$$n_M^{mod}(x) = \frac{2^{2M-1} Z^{4M/3}}{\pi M^{2M+3}((M-1)!)^2} x^{2(M-1)} \exp\left(-\frac{2}{M} Z^{2/3} x + \gamma x^{-0.855 Z^{0.065}} \right) \tag{3.21}$$

$$\gamma = \eta^{0.855 Z^{0.065}} \left[\frac{2}{M} Z^{2/3} + \log(\zeta) \right] \tag{3.22}$$

$$\zeta = \frac{2^{5/2 - 2M}}{3\pi} \left(\frac{1}{\eta} - \frac{1}{x_F} \right)^{3/2} M^{2M+3}((M-1)!)^2 Z^{-\frac{4}{3}M} \eta^{-2M+2} \tag{3.23}$$

for $x \in (\eta, \infty)$. The value of γ has been chosen particularly so that

$$\lim_{x \to \eta^+} \left[n_M^{mod}(x) - n^{TF}(x) \right] = 0 \tag{3.24}$$

which provides continuity of our model at $x = \eta$. It is important to note that by adding this second term within the exponential that the argument within the exponential does not scale in a simple fashion. Hence, this 'outer region' may actually embody two different regions in the non-interacting atom that scale differently and combine the two of them into what resembles a complete expression of the exact density on (η, ∞).
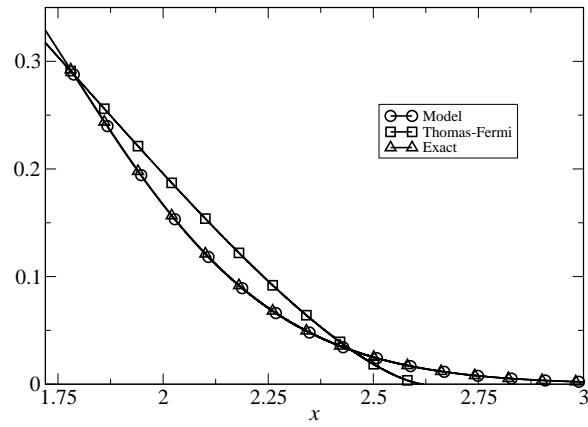
Figure 3.6: $4\pi x^2 n_5^{mod}(x)$ plotted in the outer region as a model for $4\pi x^2 n_5(x)$ as an improvement over the Thomas-Fermi approximation.
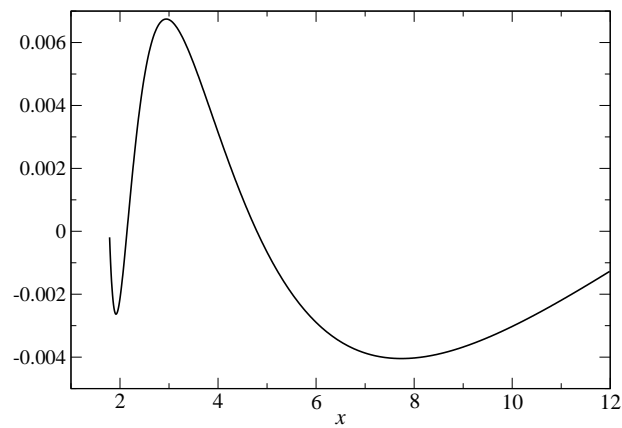
Figure 3.7: The relative difference $1 - n_5^{mod}(x)/n_5(x)$ in the outer region.

3.5 Complete Model

Now that each region has been modeled, we have a complete piecewise model for the density of the non-interacting atom, $\{n_M^{mod}(x)\}$. Once again, exact convergence to the hydrogenic density, ρ^H, does not occur, however we do have a notion of 'near convergence' since $\lim_{Z \to \infty} n_M^{mod}(Z^{-2/3}x) \to \rho^H(x)$ as $x \to 0$. Also, we cannot determine a bound for the error of our model that would better than the error for the Thomas-Fermi density due to the fact that the estimation for the frequency of the oscillation for $\{\xi_M\}$ can become completely out of phase in the intermediate region. Our model is continuous at $x = \eta$ and 'nearly continuous' at $x = \beta$ since $n_M(\beta) \approx n_M^{mod}(\beta)$. As for the normalization for our model, we have on this particular scaling,

$$1 = \int n_M(x)dx = \int n^{TF}(x)dx \approx \int n_M^{mod}(x)dx \qquad (3.25)$$

because we have $\int \left(n^{TF}(x)dx - n_M^{mod}(x) \right) \approx 0$. For the most part, many of the important properties of the exact density are met by the model, which include Kato's cusp condition at the nucleus and exponential decay for large x, but others are only 'nearly' met as means to keep our model relatively simple in construction. In turn, this provides a relatively accurate overall model, which holds well for the non-interacting Helium, which has the largest deviation from its Thomas-Fermi approximation as shown in Fig.3.9, but not quite for larger M where the oscillation of the model can become out of phase for particular values of x.

It is important to note that there is a dependence on both M and Z in the model, and that both variables can be expressed in terms of one another. So, if a closed form of $n_\infty(x)$ is achieved, it remains likely that some expressions in our model in terms of Z may be found as more accurate expressions in terms of M and vice versa.
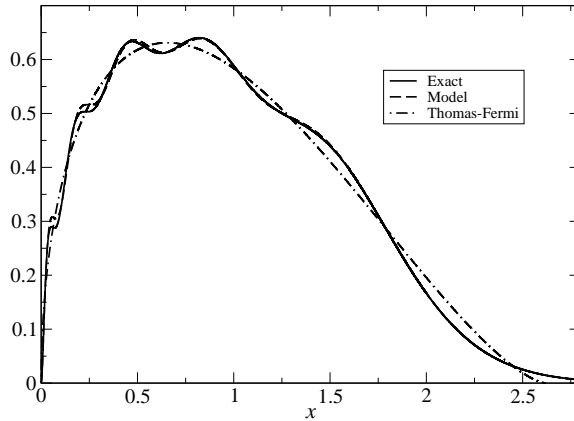
Figure 3.8: The full piecewise model $4\pi x^2 n_5^{mod}(x)$ plotted with the exact $4\pi x^2 n_5(x)$ as an improvement over the Thomas-Fermi approximation.
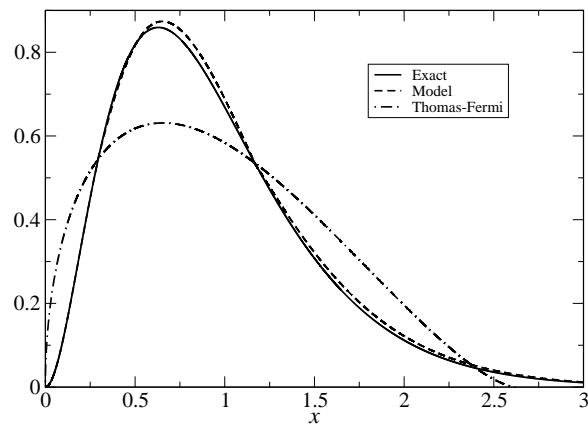
Figure 3.9: The full piecewise model $4\pi x^2 n_1^{mod}(x)$ plotted with the exact $4\pi x^2 n_1(x)$ as an improvement over Thomas-Fermi approximation.

Chapter 4

Summary

Overall, a thorough understanding of the non-interacting atom has been achieved. The energy of the system has been very well-studied with upper and lower bounds, its oscillation expressed as a smooth expansion, and many approaches have been taken to understanding the ionization energy and chemical potential. These results are rooted within an expansion of Englert's $y(N)$, which has been exposed to be a very significant factor in understanding the non-interacting atom. By extending $y(N)$ to $y(x)$ for just one particular atom, an exact energy density has been derived in terms of the density and has provided a guide for the structure for the frequency of the oscillation of the quantum correction of the density.

Since such a simple function, y, has been so useful for the non-interacting atom, it might seem appropriate to begin to study the real atom in the same fashion. However, the real system does not fill one shell at a time as more electrons are added. So, the only relatively similar function that can be for a real case would be a vector valued function $\vec{y}$ where the kth component provides how full the kth shell is. From here, it would likely be difficult to develop a closed form for the energy of the real atom in terms of a y for the real case. There could be usefulness, though, in a $\vec{y}(x)$ for the real case though as it could definitely provide information about the density and the quantum correction for the real atom as was the case with the non-interacting atom.

Once again, it is difficult to directly apply our results for the energy of the non-interacting atom to the real atom due to the electron-electron repulsion. Even so, the energies of both systems scale like $Z^{7/3}$ with a ratio of leading constants of $1.48907 \approx 3/2$, and with agreeing second terms [10]. This only further entices a search for similarities between the two systems. The exact functional developed from the energy density of the non-interacting atom may provide a fairly good approximation for the energy of the real atom. The energy oscillation could even provide insight into the oscillation of the energy in the real case. The two systems are inherently different, however this similarity between the quantized energies of each might indicate more similarity than initially thought.

By studying three different regions, the density of the non-interacting atom has been well-modeled. In the inner and outer regions, quantum conditions derived from the Schrödinger equation are used to develop forms for the density. On the intermediate region, a more involved approach was taken using the quantum correction to the Thomas-Fermi density and a limit function in the hydrogenic density. From a Kohn-Sham GF perspective, understanding this quantum correction first provides a guide for a semiclassical expansion that can provide even more accurate results than this model and can also

gateway to results for the real atom. On top of this, the model also provides a quantum correction of the density in terms of its Thomas-Fermi density, which could be particularly helpful in examining the density of the real atom. The quantum correction to the density of the real atom may have a similar expansion in terms of the real density due to a similar structure in Thomas-Fermi densities for both atoms based on their chemcial potentials as provided in Eq.(1.1).

Understanding both the energy and the density of the non-interacting atom provide no direct results for the real atom which is primarily why the non-interacting atom has been little studied as an electronic system. Now, with the energy thoroughly dealt with and the density modeled, the methodology used in understanding the non-interacting atom may provide insight or machinery that can be used for the real case, which could have a significant impact in studying the real atom.

Chapter 5

Appendix

A table of constants for Section 2.

k	a_k	b_k	c_k	d_k	α_k
0	1		$-\frac{1}{4}$	$\left(\frac{3}{2}\right)^{1/3}$	$-\frac{1}{2}\left(\frac{2}{3}\right)^{2/3}$
1	$\frac{1}{12}$	$-\frac{1}{6}$	$-\frac{1}{36}$	$-\frac{1}{2}$	$-\frac{1}{3}$
2	$-\frac{1}{5184}$	$-\frac{1}{72}$	$-\frac{7}{1296}$	$-\frac{1}{6}\left(\frac{2}{3}\right)^{1/3}$	$-\frac{7}{36}\left(\frac{2}{3}\right)^{1/3}$
3	$\frac{1}{62208}$	$-\frac{5}{2592}$	$-\frac{19}{15552}$	$-\frac{1}{216}$	$-\frac{1}{12}\left(\frac{2}{3}\right)^{2/3}$
4	$-\frac{1}{6718464}$	$-\frac{1}{3456}$	$-\frac{55}{186624}$	$-\frac{1}{3888}\left(\frac{2}{3}\right)^{2/3}$	$-\frac{1}{54}$
5	$\frac{5}{322486272}$	$-\frac{5}{124416}$	$-\frac{493}{6718464}$	$-\frac{1}{139968}\left(\frac{2}{3}\right)^{1/3}$	$\frac{1}{216}\left(\frac{2}{3}\right)^{1/3}$

Bibliography

[1] *Theory of the inhomogeneous electron gas* edited by S. Lundqvist and N.H. March. New York : Plenum Press, c1983.

[2] *Thomas-Fermi Theory Revisited* E. H. Lieb and B. Simon, Phys. Rev. Lett. **31**, 681 (1973).

[3] *Application of Thomas-Fermi model to fullerene molecule and nanotube* Yuri Kornushin, Facta Universitatis, Series: Physics, Chemistry and Technology **5**, 11-18 (2007).

[4] *Self-Consistent Equations Including Exchange and Correlation Effects* W. Kohn and L. J. Sham, Phys. Rev. **140**, A1133 (1965).

[5] *Quantum Density Oscillations in an Inhomogeneous Electron Gas* W. Kohn and L. Sham, Phys. Rev. 137, A1697 (1965).

[6] *Which functional should I choose?* D. Rappoport, N. R. M. Crawford, F. Furche, K. Burke, to appear in Computational Inorganic and Bioinorganic Chemistry, eds. E. I. Solomon, R. B. King, and R. A. Scott, Wiley, Chichester.

[7] *Semiclassical Origins of Density Functionals* Peter Elliot, Donghyung Lee, Attila Cangi, and Kieron Burke, Phys. Rev. Lett. **100**, 256406 (2008).

[8] *On a Mechanical Theorem Applicable to Heat* Clausius, RJE, Philosophical Magazine, Ser. 4 **40**: 120-127 (1870).

[9] *Semiclassical Theory of Atoms* Berthold-Georg Englert. Lecture Notes in Physics, Volume 300. Published by Springer-Verlag (Berlin Heidelberg New York), 1988.

[10] *Thomas-Fermi model: The leading correction* J. Schwinger, Phys. Rev. A **22**, 1827 (1980);

[11] *Atomic-binding-energy oscillations* Berthold-Georg Englert and Julian Schwinger, Phys. Rev. A **32**, 47 - 63 (1985)

[12] *Electron density near the nucleus of a large atom* Heilmann, Ole J. and Lieb, Elliot H, Phys Rev. A. **3628**, (1995).

[13] *On the eigenfunctions of many-particle systems in quantum mechanics* T. Kato, Comm. Pure Appl. Math. **10**, 151 (1957).

[14] *"Schrödinger inequalities" and asymptotic behavior of the electron density of atoms and molecules* Maria Hoffmann-Ostenhof and Thomas Hoffmann-Ostenhof, Phys. Rev. A **16**, 1782 (1977)

[15] *Asymptotic behavior of the ground-state charge density in atoms* Yoram Tal, Physical Review A **18** 1781 (1978)